Co-expression of ABCB1 and ABCG2 in a Cell Line Model Reveals Both Independent and Additive Transporter Function

Andrea N. Robinson, Bethelihem G. Tebase, Sonia C. Francone, Lyn M. Huff, Hanna Kozlowski, Dominique Cossari, Jung-Min Lee, Dominic Esposito, Robert W. Robey, Michael M. Gottesman

Laboratory of Cell Biology (A.N.R., B.G.T., S.C.F., L.M.H., H.K., D.C., R.W.R., M.M.G.) and Women's Malignancies Branch (J.-M.L), National Institutes of Health, Center for Cancer Research, National Cancer Institute, Bethesda, Maryland

Protein Expression Laboratory, Frederick National Laboratory for Cancer Research, Frederick, MD (D.E.)

Running Title: Co-expression of ABCB1 and ABCG2 in a cell line model

Address correspondence to:

Michael M. Gottesman, M.D.
Laboratory of Cell Biology
National Cancer Institute, NIH
37 Convent Drive, Room 2108
Bethesda, MD 20892
Email: mgottesman@nih.gov

Text pages: 29
Number of tables: 2
Figures: 7
References: 33
Words in the Abstract: 247
Introduction: 695
Discussion: 943

Non-standard abbreviations:
AML, acute myelogenous leukemia; AUC, area under the curve; BBB, blood-brain barrier; FBS, fetal bovine serum; FTC, fumitremorgin; MEF, mouse embryonic fibroblast; MEM, Eagle's minimum essential medium; VAL, valspodar; PhA, pheophorbide a

ABSTRACT

Although overexpression of multiple ATP-binding cassette transporters has been reported in clinical samples, few studies have examined how co-expression of multiple transporters affected resistance to chemotherapeutic drugs. We therefore examined how co-expression of ABCB1 (P-glycoprotein) and ABCG2 contribute to drug resistance in a cell line model. HEK-293 cells were transfected with vector encoding full-length *ABCB1*, *ABCG2*, or a bicistronic vector containing both genes, each under the control of a separate promoter. Cells transfected with both transporters (B1/G2 cells) demonstrated high levels of both transporters and uptake of both the ABCB1-specific substrate rhodamine 123 and the ABCG2-specific substrate pheophorbide a was reduced when examined by flow cytometry. B1/G2 cells were also cross-resistant to the ABCB1 substrate doxorubicin, the ABCG2 substrate topotecan, as well as mitoxantrone and the cell cycle checkpoint kinase 1 inhibitor prexasertib, both of which were found to be substrates of both ABCB1 and ABCG2. When B1/G2 cells were incubated with both rhodamine 123 and pheophorbide a, transport of both compounds was observed, suggesting that ABCB1 and ABCG2, when co-expressed, can function independently to transport substrates. ABCB1 and ABCG2 also functioned additively to transport the common fluorescent substrates mitoxantrone and BODIPY®-prazosin, as it was necessary to inhibit both transporters to prevent efflux from B1/G2 cells. ABCG2 expression was also found to decrease the efficacy of the ABCB1 inhibitor tariquidar in B1/G2 cells. Thus, ABCB1 and ABCG2 can independently and additively confer resistance to substrates, underscoring the need to inhibit multiple transporters when they are co-expressed.

INTRODUCTION

Overexpression of ABCB1 (P-glycoprotein, encoded by the *ABCB1* gene) or ABCG2 is

known to confer resistance to multiple chemotherapeutic drugs, including many targeted

therapies under clinical development (Robey et al., 2018). Additionally, these transporters are

known to limit oral bioavailability, as both are expressed in the gastrointestinal tract (Thiebaut

et al., 1987; Maliepaard et al., 2001; Fetsch et al., 2006). In knockout models, mice deficient in

both *Abcb1a* and *Abcb1b* (the murine homologs of human *ABCB1,* previously known as *mdr1a*

and *mdr1b*) demonstrate increased oral bioavailability of ABCB1 substrates such as taxol

compared to wild-type mice (Sparreboom et al., 1997). Similar results have been found with the

ABCG2 substrate sulfasalazine, where mice deficient in *Abcg2* had higher plasma drug levels

after oral administration of the drug compared to control mice (Zaher et al., 2006).

It has been demonstrated that both ABCB1 and ABCG2 can limit the oral bioavailability

of common substrates. Upon oral administration of the mutant BRAF inhibitor vemurafenib,

plasma area under the curve (AUC) values were 1.6-fold higher in Abcb1a/1b-deficient mice and

2.3-fold higher in Abcg2-deficient mice but were 6.6-fold higher in mice deficient in both

transporters compared to wild-type controls (Durmus et al., 2012). Similarly, plasma AUCs of

the EGFR/HER-2 inhibitor afatinib were 4.2-fold, 2.4-fold and 7-fold higher in Abcg2, Abcb1a/1b

and double knockout mice, respectively, compared to wild-type mice (van Hoppe et al., 2017),

thus suggesting that both transporters contribute to decreased oral bioavailability of

substrates.

Additionally, ABCB1 and ABCG2 are co-expressed in the brain capillaries that form the

blood-brain barrier (BBB) (Cooray et al., 2002; Fetsch et al., 2006) and serve to keep toxins and

some chemotherapeutic agents out of the brain (Robey et al., 2010). Mouse knockout models

point to a compensatory and cooperative role for ABCB1 and ABCG2 at the BBB. Brain

concentrations of the PARP inhibitor rucaparib were increased by 2-fold, 5.2-fold, and 32.6-fold

in mice deficient in Abcg2, Abcb1a/1b or both transporters, respectively, compared to wild-type

controls, suggesting a cooperative role for the two transporters at the BBB (Durmus et al.,

2015b). ABCB1 and ABCG2 were found to cooperatively exclude the JAK1/2 inhibitor

momelotinib from the brain, as 8 h after oral administration of the drug, mice deficient in

Abcg2, Abcb1a/b or Abcg2;Abcb1a/b were found to have 6.5-fold, 3-fold, or 48-fold higher

brain levels compared to controls (Durmus et al., 2013). This apparent synergism from deleting

both of the murine homologs for ABCB1 and ABCG2 results from the fact that transport due to

ABCB1 and ABCG2 is much higher than passive diffusion of the drugs across the BBB (Kusuhara

and Sugiyama, 2009; Kodaira et al., 2010). Coadministration of the dual ABCB1/ABCG2 inhibitor

elacridar resulted in significantly increased brain levels of the kinase inhibitors tandutinib (Yang

et al., 2010), pazopanib (Minocha et al., 2012) and sunitinib (Tang et al., 2010). ABCB1 and

ABCG2 are thus major obstacles to overcome when treating brain cancers or metastases to the

brain.

ABCB1 and ABCG2 are found to be co-expressed in some cancers, particularly leukemia.

Wilson and colleagues obtained gene expression profiles of 170 pretreated samples of acute

myelogenous leukemia (AML) by microarray analysis (Wilson et al., 2006). Using unsupervised

clustering, the patients clustered into 6 groups; the cluster characterized by the highest levels

of resistant disease showed increased expression of ABCB1 and ABCG2 (Wilson et al., 2006).

Profiling 380 drug-resistance related genes in a set of 11 paired samples obtained at diagnosis

and again at relapse identified 2 patients with increases in both ABCB1 and ABCG2 at relapse (Patel et al., 2013). Liu et al examined expression of ABCB1, ABCB4, ABCC1, ABCC4 and ABCG2 in bone marrow mononuclear cells from 96 de novo AML patients and found that co-expression of multiple transporters was associated with worse prognosis (Liu et al., 2018). Expression of multiple transporters may therefore confer greater resistance to chemotherapy than expression of a single transporter.

Despite evidence suggesting a cooperative and potentially compensatory role for ABCB1 and ABCG2, few studies have addressed how these transporters might be working together to render chemotherapy less effective. We thus generated HEK293 cell lines that express both transporters and find that the transporters function both independently and additively to transport substrates.

MATERIALS AND METHODS

Chemicals. Doxorubicin, mitoxantrone, paclitaxel, etoposide, and rhodamine 123 were purchased from Sigma-Aldrich (St. Louis, MO). SN-38 and topotecan were from LKT Laboratories (St. Paul, MN). Valspodar was obtained from Apex Biotechnology (Houston, TX). PHA was purchased from Frontier Scientific (Logan, UT). Zeocin was from InvivoGen (San Diego, CA) and prexasertib from Selleck Chemicals (Houston, TX). BODIPY-prazosin was obtained from Life Technologies (Eugene, OR). Tariquidar was a kind gift of Xenova Group (Slough, UK). Fumitremorgin (FTC) was synthesized by the NIH Chemical Biology Laboratory, Bethesda, MD.

Cell lines. Human embryonic kidney cells (HEK293) were obtained from ATCC (Manassas, VA)

and cultured in MEM (Eagle's minimum essential medium) (Gibco/Life Technologies, Carlsbad,

CA) with 10% fetal bovine serum (FBS), 1% glutamine, and 1% penicillin. Cells were transfected

with empty vector with zeocin resistance alone, vectors encoding full-length human *ABCB1* or

ABCG2, or a bicistronic vector in which each gene is under the control of a separate CMV

promoter. *ABCB1* and *ABCG2* expression constructs were generated by Gateway cloning using

human cDNA templates. Both genes were cloned with Kozak translational initiation sites prior

to the initiator methionine and stop codons at the 3' end. Genes were amplified by low-cycle

PCR using primers with Gateway recombination sites, and Entry clones were generated using BP

recombination under the manufacturer's standard conditions (ThermoFisher, Waltham,

MA). Entry clones were fully sequence verified and the genes were transferred by Gateway LR

recombination into pDest-760, a mammalian expression vector based on the pcDNA3.1-zeo

vector (ThermoFisher) which contains a moderate strength CMV promoter and carries a zeocin

resistance marker. A control construct was generated in which a stuffer fragment of non-

coding DNA was inserted into pDest-760 to serve as a control for protein expression constructs.

A bicistronic *ABCB1/ABCG2* expression vector was generated using combinatorial

Multisite Gateway (Wall et al., 2014) in which *ABCB1* was cloned into a Gateway Entry clone

flanked by attB4 and attB5 sites. This product was then recombined with a CMV13 promoter

fragment flanked with attB5 and attB1 sites and the standard *ABCG2* Entry clone previously

generated. This recombination was carried out in the pDest-301 Multisite vector (attR4/attR2)

which was derived from the pcDNA3.1-zeo vector. The final construct is of the form of

CMV3.1p>*ABCB1*>CMV13p>*ABCG2*, where the *ABCB1* gene is 5' to the *ABCG2* gene, leading to bicistronic production of the two genes from a single expression construct.

After transfection of cells, clones resistant to zeocin were collected and expression of the various transporters was verified by flow cytometry, as outlined below. Selected clones were maintained in 250 µg/ml zeocin. The positive control HEK-293 cell lines transfected with pcDNA vector containing full-length *ABCB1* (MDR-19) or *ABCG2* (R-5) were previously described (Robey et al., 2003).

Flow Cytometry. Cell surface expression of ABCB1 and ABCG2 was verified using phycoerythrin-labeled UIC2 antibody or phycoerythrin-labeled 5D3 antibody (both from Thermo-Fisher) respectively, and corresponding isotype control antibodies. Briefly, cells were trypsinized and incubated with antibodies at saturating concentrations in the absence of substrates or inhibitors in 2% BSA for 20 minutes at room temperature. Cells were washed twice with phosphate-buffered saline (PBS), then analyzed by flow cytometry.

ABCB1- or ABCG2-mediated transport was examined by a flow cytometry efflux assay (Robey et al., 2004). Trypsinized cells were resuspended in complete medium (phenol red-free IMEM with 10% FBS, 1% glutamine, and 1% penicillin) containing 2 µM PhA or 0.5 mg/ml rhodamine 123, in the presence or absence of 2.5 µM of ABCB1 inhibitor valspodar (positive control for ABCB1 inhibition), or 10 µM of the ABCG2 inhibitor fumitremorgin C (FTC, positive control for ABCG2 inhibition), and incubated for 30 minutes at 37˚C in 5% CO_2. Cells were then washed and incubated for 1 hour at 37˚C in substrate-free complete media continuing with or

8

without valspodar or FTC. Subsequently, cells were washed twice with cold PBS and placed on ice until analyzed.

Samples were analyzed by a FACSCanto II flow cytometer (Becton Dickinson Bioscience, San Jose, CA). Phycoerythrin fluorescence was detected by a 488-nm argon laser with a 585-nm bandpass filter. PhA and mitoxantrone fluorescence were detected using a 633-nm HeNe laser with a 660-nm bandpass filter. Rhodamine 123 was detected with a 488-nm argon laser with a 530-nm bandpass filter. At least 10,000 events were collected for each sample.

Cytotoxicity assays. Briefly, trypsinized cells were seeded in an opaque white 96-well plate (5000 cells/well) and allowed to attach overnight at 37°C in 5% CO_2. Anti-cancer compounds were added at various concentrations and incubated for 72 h at 37°C in 5% CO_2. Cell viability was determined using CellTiter-Glo (Promega, Madison, WI) reagent according to the manufacturer's instructions. Luminescence was subsequently read on a Tecan Infinite M200 Pro microplate reader (Tecan Group, Morrisville, NC). Each determination was performed in triplicate.

Immunoblot Analysis. Cell lysates (30 μg) were heated to 37° for 20 minutes then subjected to electrophoresis on a premade 4-12% bis- tris gel and transferred to a nitrocellulose membrane. Subsequently the blot was blocked with Odyssey Blocking Buffer (Li-COR Lincoln, NE) for one hour at room temperature, then probed overnight with mouse monoclonal anti-GAPDH (American Researchg Products, Waltham, MA, 1:8000), the anti-Pgp antibody C219 (Signet Laboratories, Dedham, MA, 1:250), and anti-ABCG2 antibody, BXP-21 (Kamiya Biomedical,

9

Seattle, WA, 1:250). The blot was then incubated with a goat anti-mouse secondary antibody

tagged with a near infra-red fluorochrome and fluorescence was measured using the LiCor

ODYSSEY CLx (LI-COR).

RESULTS

Characterization of a transfected cell line engineered to co-express ABCB1 and ABCG2.

Despite the fact that ABCB1 and ABCG2 are co-expressed in many cancers (Robey et al., 2018),

few studies have examined the effect that co-expression has on drug resistance and inhibitor

efficacy. To that end, we transfected HEK-293 cells to express ABCB1 and ABCG2 individually as

well as together, using a novel bicistronic vector to express both *ABCB1* and *ABCG2*. After

transfection, we examined transporter expression in the clones and selected a set in which the

cells transfected to express both transporters expressed ABCB1 and ABCG2 at levels similar to

those of cells that were transfected with the transporter genes individually. Our initial screen of

clones examined surface expression by flow cytometry and we selected a set based on similar

staining with the UIC2 and 5D3 antibodies that detected ABCB1 or ABCG2, respectively. Cells

expressing both ABCB1 and ABCG2 (B1/G2) demonstrated similar levels of transporter

expression comparable to that of the clones that express ABCB1 (B1) or ABCG2 (G2) individually

(Fig. 1A), although levels of both ABCB1 and ABCG2 in B1/G2 cells were somewhat lower than

the individually transfected cell lines. The G2 cell line expresses a low level of ABCB1 that is

attributed to endogenous levels in the parental HEK293 cells. Empty vector transfected cells

(PEL) also express low levels of ABCB1 and no ABCG2. Western blot analysis also demonstrated

comparable levels of ABCB1 and ABCG2 in the double transfected cell line as compared to cells

10

expressing only one transporter, with empty vector transfected cells expressing no detectable

protein from either transporter (Fig. 1B). MDR-19 and R-5 cells were used as positive controls

for ABCB1 and ABCG2, respectively, in the immunoblot assay.

To confirm that each of the proteins was functional and capable of transporting

substrates, we examined the transport of the fluorescent substrates rhodamine 123 and

pheophorbide a, specific substrates of ABCB1 and ABCG2, respectively. As can be observed in

Fig. 2, B1/G2 cells that co-express ABCB1 and ABCG2 efflux pheophorbide a to a similar degree

as the G2 cells that express only ABCG2 (blue histogram). Similarly, B1/G2 cells demonstrate a

similar decrease in rhodamine 123 fluorescence as B1 cells that express only ABCB1. Thus,

levels of functional ABCB1 appear to be similar in the B1 and B1/G2 cells and the levels of

functional ABCG2 appear to be similar in the G2 and B1/G2 cell lines based on comparable

transport of specific substrates.

We also performed three-day cytotoxicity assays on B1, G2 and B1/G2 cells to verify that

B1/G2 cells were resistant to drugs that are substrates of both ABCB1 and ABCG2. We

performed cytotoxicity assays with mitoxantrone, doxorubicin, topotecan, and prexasertib. As

shown in Fig. 3, we found that both B1 and B1/G2 cell lines were more resistant to doxorubicin

than G2 cells, that G2 and B1/G2 cells were more resistant to topotecan than B1 cells, and that

all transporter-expressing cells displayed high levels of resistance to the common substrate

mitoxantrone. We also found that the cell cycle checkpoint kinase 1 (CHK1) inhibitor

prexasertib is transported by both ABCB1 and ABCG2, as all transporter-expressing cells were

resistant to the drug. Relative resistance values are summarized in Table 1. Despite expressing

both transporters, B1/G2 cells did not appear to have greater resistance to mitoxantrone or

prexasertib than the cells expressing the transporters individually. This is most likely due to the

fact that levels of the individual transporters are somewhat lower in B1/G2 cells compared to

expression in the cells expressing the transporters individually (see Fig. 1). After verifying that

B1/G2 cells express high levels of functional ABCB1 and ABCG2, we performed further

experiments on the cells to determine the contribution of each transporter to drug resistance.

ABCB1 and ABCG2 can independently efflux transporter-specific fluorescent substrates. We

next examined whether ABCB1 and ABCG2 can operate independently of each other by

examining transport of specific substrates in B1/G2 cells and compared this to transport in B1

and G2 cells. We performed efflux studies in a manner similar to those done for Fig. 2, except

we exposed the B1/G2 cells to both PhA and rhodamine 123 simultaneously, in the presence or

absence of the inhibitors valspodar (VAL) and FTC alone or in combination (FTC/VAL). Substrate

efflux was monitored by examining rhodamine fluorescence using the 488 nm laser (488 nm)

and PHA using the 650 nm laser (650 nm) so as to avoid spectral overlap of the substrates. We

also performed the assay with the substrates individually, using valspodar with rhodamine 123

(RHO + VAL) and FTC with PhA (PHA + FTC). As can be observed in Fig. 4A, when cells were

incubated with rhodamine alone (top row) or PhA and rhodamine together (second row),

comparable rhodamine efflux is observed in the B1 and B1/G2 cells; only a slight amount of

efflux is observed in the G2 cells. Further, no transport is observed in B1 cells when cells were

incubated with PHA alone (top row) or PhA and rhodamine together (second row), as evidenced

by the nearly overlapping blue and orange histograms (Fig. 4B). However, G1 and B1/G2 cells

transport PhA similarly, as shown by the comparable distance between the blue and orange

histograms (Fig. 4B). These studies demonstrate that B1 and G2 can function independently of one another to transport specific substrates when co-expressed.

For substrates common to both transporters, inhibiting either ABCB1 or ABCG2 when they are co-expressed only partially prevents transport. We next examined the transport of common fluorescent substrates in the B1, G2 and B1/G2 cells. We selected mitoxantrone and BODIPY-prazosin, fluorescent compounds that are transported by both ABCB1 and ABCG2 (Litman et al., 2000; Robey et al., 2008). In this experiment, B1, G2 or B1/G2 cells were incubated with mitoxantrone or BODIPY-prazosin in the presence or absence of valspodar (VAL), FTC or both inhibitors as outlined above in the Materials and Methods. Results with mitoxantrone or BODIPY-prazosin are shown in rows one and two of Fig. 5, respectively. As observed in the top row of Fig. 5, virtually no efflux is prevented when B1 cells are incubated in mitoxantrone in the presence of FTC (green histogram), and this histogram overlaps with the histogram when cells are incubated in mitoxantrone alone (blue histogram). However, intracellular mitoxantrone fluorescence increases in the presence of valspodar (orange histogram), as well as when FTC and valspodar are added together with mitoxantrone (purple histogram). In the case of the G2 cells, valspodar added to the mitoxantrone (orange histogram) does little to increase fluorescence compared to cells incubated with mitoxantrone alone (blue histogram). Only FTC (green histogram) is able to increase intracellular mitoxantrone levels and this overlaps with cells incubated with mitoxantrone in the presence of both inhibitors (purple histogram). B1/G2 cells incubated with mitoxantrone in the presence of valspodar (orange histogram) or FTC (green histogram) do not appreciably increase fluorescence compared to

cells incubated with mitoxantrone alone (blue histogram). Only when B1/G2 cells are incubated

with valspodar and FTC together (purple histogram) is efflux maximally inhibited.

Similar results were found with BODIPY-prazosin (Fig. 5, bottom row). In B1 cells

incubated with BODIPY-prazosin, only valspodar (orange histogram) or both valspodar and FTC

(purple histogram) are able to increase intracellular prazosin levels to levels higher than those

of cells incubated with prazosin alone (blue histogram). In the case of G2 cells, valspodar

(orange histogram) does slightly increase prazosin fluorescence compared to cells incubated

with prazosin alone (blue histogram), most likely due to inhibition of the low levels of ABCB1

expressed by HEK293 cells. However, maximal inhibition is observed when cells are incubated

in prazosin with FTC (green histogram) or both valspodar and FTC (purple histogram). Finally, in

the B1/G2 cells, incubating cells with prazosin in the presence of valspodar (orange histogram)

or FTC (green histogram) have equal effects on increasing intracellular fluorescence, but

maximal inhibition is only observed when both inhibitors are added (purple histogram). These

results indicate that both ABCB1 and ABCG2 must be inhibited to completely prevent transport

of common substrates when both transporters are expressed.

In cytotoxicity assays, ABCB1 and ABCG2 display substrate-specific additive activity. In order

to determine the effects of ABCB1 and ABCG2 co-expression on resistance to long-term

exposure to common substrates, 3-day cytotoxicity assays were performed on empty-vector

transfected and B1/G2-transfected clones. We chose mitoxantrone and prexasertib, which are

transported by both transporters relatively well, as previously shown. The contribution of each

transporter to resistance to the drugs was determined by performing cytotoxicity assays in the

absence or presence of valspodar and FTC alone or in combination. As shown in Fig. 6A, B1/G2

cells are approximately 40-fold more resistant to mitoxantrone compared to B1/G2 cells

incubated with both valspodar and FTC. When the cells are incubated with mitoxantrone in the

presence of the ABCG2 inhibitor FTC, the cells are only about 30-fold more resistant; when the

cells are incubated with mitoxantrone in the presence of the ABCB1 inhibitor valspodar, the

cells are approximately 20-fold more resistant. This suggests that the transporters are

conferring additive resistance to mitoxantrone. This was confirmed in another B1/G2 clone (F6)

(Suppplemental Figure 1A), in which cells were 50-fold resistant to mitoxantrone in the absence

of inhibitors compared to the presence of both valspodar and FTC; cells were 8-fold resistant to

mitoxantrone in the presence of valspodar and 33-fold resistant in the presence of FTC, again

suggesting additive resistance (Supplemental Figure 1B and Supplemental Table 1). The same

was true for prexasertib (Fig. 6B), as B1/G2 cells were approximately 10-fold more resistant to

prexasertib compared to B1/G2 cells incubated with prexasertib in the presence of valspodar

and FTC. When B1/G2 cells were incubated with prexasertib in the presence of FTC, resistance

was 8-fold greater; when the cells were incubated with prexasertib and valspodar, resistance

was only 6-fold more. Again, we conclude that ABCB1 and ABCG2 must both be inhibited in

order to completely overcome resistance to drugs that are substrates of both transporters in

cells in which both transporters are expressed.

ABCG2 expression decreases efficacy of the ABCB1 inhibitor tariquidar in cells expressing

both transporters. Previous work in our laboratory demonstrated that the ABCB1 inhibitor

tariquidar is a substrate of ABCG2 (Kannan et al., 2011), potentially signifying that co-expression

15

of ABCG2 could alter the ability of tariquidar to inhibit ABCB1. We thus examined rhodamine

efflux in B1/G2 cells incubated with increasing amounts of tariquidar and compared this to

efflux in B1 cells that express only ABCB1 to see if ABCG2 expression had any impact on the

ability of tariquidar to inhibit ABCB1. The ABCG2 inhibitor valspodar was used as a positive

control. As seen in Fig. 7A, the ability of tariquidar to inhibit ABCB1 was affected by the

presence of ABCG2, as the ability of tariquidar to inhibit ABCB1 at the 100 nM and 250 nM

concentrations was different in ABCB1-overexpressing cells (Figure 7A) and cells expressing

both ABCB1 and ABCG2 (Figure 7B). When the fluorescence of cells incubated with rhodamine

in the presence of valspodar was assigned a value of 100%, the percent inhibition in cells

incubated with rhodamine the presence of of 100 nM and 250 nM tariquiar was significantly

different in B1 and B1/G2 cells (Fig. 7C). Thus, in drug-resistant cancer cells, co-expression of

ABCG2 may decrease the ability of tariquidar to inhibit ABCB1.

DISCUSSION

In this study, we attempted to delineate how ABCB1 and ABCG2 contribute to drug

resistance when co-expressed in a cell line model. We used a novel bicistronic vector to develop

the B1/G2 cell line that co-expresses both transporters. In the B1/G2 cell line, we find that

ABCB1 and ABCG2 are both fully functional and readily transport known substrates. In flow

cytometry studies, the transporters are capable of transporting specific substrates such as

rhodamine 123 (specific for ABCB1) and PhA (specific for ABCG2) independently of each other

when exposed to the compounds simultaneously, but also act additively to transport common

substrates such as BODIPY-prazosin and mitoxantrone. In cytotoxicity assays, the transporters

appear to additively confer resistance to common substrates such as mitoxantrone and prexasertib. These results point to the need to inhibit both transporters in order to overcome resistance to drugs that are substrates of both transporters. Additionally, the transporters more than likely can confer resistance to combination chemotherapy if the components are transporter substrates. We also demonstrate that the presence of ABCG2 can decrease the efficacy of the ABCB1 inhibitor tariquidar. The frequent failure of transporter inhibitors in clinical trials may have been due to their inability to inhibit multiple transporters at clinically achievable concentrations or may be due to another transporter decreasing the efficacy of an inhibitor.

Since we found that expression of multiple transporters led to additive resistance to chemotherapy, it seems reasonable to assume that if multiple transporters were expressed at low levels, they might confer clinically meaningful levels of drug resistance. This was previously demonstrated by Allen and colleagues, who created a series of mouse embryonic fibroblasts (MEFs) that were proficient or deficient in mouse *Abcb1a/1b* and *Abcc1* expression (Allen et al., 2000). Compared to wild-type MEFs, MEFs deficient in *Abcb1a/b* expression were 16-fold, 2.4-fold, 4.7-fold, and 2.5-fold more sensitive to paclitaxel, vincristine, doxorubicin, or mitoxantrone, respectively, while cells deficient in both *Abcb1a/1b* and *Abcc1* were 22-fold, 28-fold, 7.1-fold or 4.3-fold more sensitive to the drugs, respectively (Allen et al., 2000). Thus, if a drug-resistant cell line expressed 3 different transporters that conferred only 2-fold more resistance to a drug, inhibiting only one might still lead to a cell which was 4-fold more resistant to the compound, which might be clinically meaningful. This is supported by clinical data showing that expression of multiple transporters leads to a worse clinical prognosis (Liu et al.,

2018). Inhibition of all transporters expressed by a cancer cell may thus be necessary to overcome transporter-mediated drug resistance.

We also report here for the first time that the CHK1 inhibitor prexasertib is transported by both ABCB1 and ABCG2. This is not surprising, as a number of targeted therapies have been shown to interact with one or both of the transporters (Robey et al., 2018). Some of the more recently identified transporter substrates include the fibroblast growth factor receptor AZD4547 (Kas et al., 2018), the DOT1L inhibitor pinometostat (Campbell et al., 2017), the MET inhibitor PHA-665752 (Sugano et al., 2015), and the survivin inhibitor YM-155 (Lamers et al., 2012). As most compounds that are substrates of either ABCB1 or ABCG2 generally do not cross the BBB (Durmus et al., 2015a), it does not appear that prexasertib would be able to treat cancer that has metastasized to the brain or primary brain tumors. Clinically achievable concentrations of prexasertib are in the 100-175 nM range (Brill et al., 2017).

Our model does not recapitulate knockout mouse studies in which knockout of both transporters results in greatly increased brain penetration of some chemotherapeutic agents. In the case of axitinib, brain penetration of the drug was not significantly changed in Abcg2-deficient mice compared to wild-type, while brain penetration was 4.9-fold higher in mice deficient in Abcb1a/1b and 20.7-fold higher in mice deficient in both transporters compared to wild-type mice at 4 h after oral administration (Poller et al., 2011a). Similar results were found with the JAK1/2 inhibitor momelotinib, where compared to wild-type mice, mice deficient in Abcg2 had 6.5-fold higher brain levels of momelotinib, mice deficient in ABcb1a/1b had 3.1-fold higher levels, and mice deficient in both transporters had 48.3-fold higher levels 8 h after oral administration of the drug. This suggests a synergistic role for ABCB1 and ABCG2 at the BBB,

due to the fact that the effect of the transporters on substrates is greater than passive diffusion

across the BBB (Kusuhara and Sugiyama, 2009). That we were not able to mimic the mouse

model is most likely due to the fact that HEK-293 cells do not form epithelial monolayers with

tight junctions that would limit passive diffusion. This is supported by Poller et al., who

developed a doubly-transduced MDCKII cell line that expresses human *ABCB1* and *ABCG2*

(Poller et al., 2011b). MDCKII cells are known to form monolayers with tight junctions

(Brückner and Janshoff, 2018). Poller et al. found that the inverse monolayer transport ratios of

topotecan, sorafenib, and sunitinib in MDCKII-ABCB1/ABCG2 cells without inhibition, in the

presence of Ko143 to inhibit ABCG2, in the presence of zosuquidar to inhibit ABCB1, or in the

presence of both inhibitors, closely modeled *in vivo* brain penetration of wild-type mice, mice

deficient in Abcg2, mice deficient in Abcb1a/1b, or deficient in both transporters, respectively

(Poller et al., 2011b). Our model would therefore be more applicable to to drug-resistant cancer

cells that generally do not form tight junctions and transporter monolayers.

In conclusion, we have generated a cell line model that expresses high levels of human

ABCB1 and ABCG2. The transporters appear to function independently as well as additively to

confer resistance to substrates. This cell line model may be useful in studying the role of these

transporters in cancer drug resistance.

ACKNOWLEDGEMENTS

nor does mention of trade names, commercial products, or organizations imply endorsement

by the U.S. Government.

AUTHOR CONTRIBUTIONS

Participated in research design: Robey, Gottesman

Conducted experiments: Robinson, Tebase, Francone, Huff, Kozlowski, Cossari, Robey

Contributed new reagents or analytic tools: Lee, Esposito

Performed data analysis: Robinson, Robey, Gottesman

Wrote or contributed to writing the manuscript: Robinson, Robey, Gottesman

REFERENCES

Allen JD, Brinkhuis RF, van Deemter L, Wijnholds J, and Schinkel AH (2000) Extensive contribution of the multidrug transporters P-glycoprotein and Mrp1 to basal drug resistance. *Cancer Res* **60:**5761-5766.

Brill E, Yokoyama T, Nair J, Yu M, Ahn YR, and Lee JM (2017) Prexasertib , a cell cycle checkpoint kinases 1 and 2 inhibitor, increases in *vitro t*oxicity of PARP inhibition by preventing Rad51 foci formation in BR*CA w*ild type high-grade serous ovarian cancer. *Oncotarget* **8:**111026-111040.

Brückner BR and Janshoff A (2018) Importance of integrity of cell-cell junctions for the mechanics of confluent MDCK II cells. *Sci Rep* **8:**14117.

Campbell CT, Haladyna JN, Drubin DA, Thomson TM, Maria MJ, Yamauchi T, Waters NJ, Olhava EJ, Pollock RM, Smith JJ, Copeland RA, Blakemore SJ, Bernt KM, and Daigle SR (2017) Mechanisms of Pinometostat (EPZ-5676) Treatment-Emergent Resistance in. *Mol Cancer Ther* **16:**1669-1679.

Cooray HC, Blackmore CG, Maskell L, and Barrand MA (2002) Localisation of breast cancer resistance protein in microvessel endothelium of human brain. *Neuroreport* **13:**2059-2063.

Durmus S, Hendrikx JJ, and Schinkel AH (2015a) Apical ABC transporters and cancer chemotherapeutic drug disposition. *Adv Cancer Res* **125:**1-41.

Durmus S, Sparidans RW, van Esch A, Wagenaar E, Beijnen JH, and Schinkel AH (2015b) Breast cancer resistance protein (BCRP/ABCG2) and P-glycoprotein (P-GP/ABCB1) restrict oral availability and brain accumulation of the PARP inhibitor rucaparib (AG-014699). *Pharm Res* **32:**37-46.

Durmus S, Sparidans RW, Wagenaar E, Beijnen JH, and Schinkel AH (2012) Oral availability and brain penetration of the B-RAFV600E inhibitor vemurafenib can be enhanced by the P-GLYCOprotein (ABCB1) and breast cancer resistance protein (ABCG2) inhibitor elacridar. *Mol Pharm* **9:**3236-3245.

Durmus S, Xu N, Sparidans RW, Wagenaar E, Beijnen JH, and Schinkel AH (2013) P-glycoprotein (MDR1/ABCB1) and breast cancer resistance protein (BCRP/ABCG2) restrict brain accumulation of the JAK1/2 inhibitor, CYT387. *Pharmacol Res* **76:**9-16.

Fetsch P, Abati A, Litman T, Morisaki K, Honjo Y, Mittal K, and Bates S (2006) Localization of the ABCG2 mitoxantrone resistance-associated protein in normal tissues. *Cancer Lett* **235:**84-92.

Kannan P, Telu S, Shukla S, Ambudkar SV, Pike VW, Halldin C, Gottesman MM, Innis RB, and Hall MD (2011) The "specific" P-glycoprotein inhibitor Tariquidar is also a substrate and an inhibitor for breast cancer resistance protein (BCRP/ABCG2). *ACS Chem Neurosci* **2:**82-89.

Kas SM, de Ruiter JR, Schipper K, Schut E, Bombardelli L, Wientjens E, Drenth AP, de Korte-Grimmerink R, Mahakena S, Phillips C, Smith PD, Klarenbeek S, van de Wetering K, Berns A, Wessels LFA, and Jonkers J (2018) Transcriptomics and Transposon Mutagenesis Identify Multiple Mechanisms of Resistance to the FGFR Inhibitor AZD4547. *Cancer Res* **78:**5668-5679.

Kodaira H, Kusuhara H, Ushiki J, Fuse E, and Sugiyama Y (2010) Kinetic analysis of the cooperation of P-glycoprotein (P-gp/Abcb1) and breast cancer resistance protein (Bcrp/Abcg2) in limiting the brain and testis penetration of erlotinib, flavopiridol, and mitoxantrone. *J Pharmacol Exp Ther* **333:**788-796.

Kusuhara H and Sugiyama Y (2009) In vitro-in vivo extrapolation of transporter-mediated clearance in the liver and kidney. *Drug Metab Pharmacokinet* **24:**37-52.

Lamers F, Schild L, Koster J, Versteeg R, Caron HN, and Molenaar JJ (2012) Targeted BIRC5 silencing using YM155 causes cell death in neuroblastoma cells with low ABCB1 expression. *Eur J Cancer* **48:**763-771.

Litman T, Brangi M, Hudson E, Fetsch P, Abati A, Ross DD, Miyake K, Resau JH, and Bates SE (2000) The multidrug-resistant phenotype associated with overexpression of the new ABC half-transporter, MXR (ABCG2). *J Cell Sci* **113:**2011-2021.

Liu B, Li LJ, Gong X, Zhang W, Zhang H, and Zhao L (2018) Co-expression of ATP binding cassette transporters is associated with poor prognosis in acute myeloid leukemia. *Oncol Lett* **15:**6671-6677.

Maliepaard M, Scheffer GL, Faneyte IF, van Gastelen MA, Pijnenborg AC, Schinkel AH, van De Vijver MJ, Scheper RJ, and Schellens JH (2001) Subcellular localization and distribution of the breast cancer resistance protein transporter in normal human tissues. *Cancer Res* **61:**3458-3464.

Minocha M, Khurana V, Qin B, Pal D, and Mitra AK (2012) Enhanced brain accumulation of pazopanib by modulating P-gp and Bcrp1 mediated efflux with canertinib or erlotinib. *Int J Pharm* **436:**127-134.

Patel C, Stenke L, Varma S, Lindberg ML, Björkholm M, Sjöberg J, Viktorsson K, Lewensohn R, Landgren O, Gottesman MM, and Gillet JP (2013) Multidrug resistance in relapsed acute myeloid leukemia: evidence of biological heterogeneity. *Cancer* **119:**3076-3083.

Poller B, Iusuf D, Sparidans RW, Wagenaar E, Beijnen JH, and Schinkel AH (2011a) Differential impact of P-glycoprotein (ABCB1) and breast cancer resistance protein (ABCG2) on axitinib brain accumulation and oral plasma pharmacokinetics. *Drug Metab Dispos* **39:**729-735.

Poller B, Wagenaar E, Tang SC, and Schinkel AH (2011b) Double-transduced MDCKII cells to study human P-glycoprotein (ABCB1) and breast cancer resistance protein (ABCG2) interplay in drug transport across the blood-brain barrier. *Mol Pharm* **8:**571-582.

Robey RW, Honjo Y, Morisaki K, Nadjem TA, Runge S, Risbood M, Poruchynsky MS, and Bates SE (2003) Mutations at amino acid 482 in the ABCG2 gene affect substrate and antagonist specificity. *Br J Cancer* **89:**1971-1978.

Robey RW, Massey PR, Amiri-Kordestani L, and Bates SE (2010) ABC transporters: unvalidated therapeutic targets in cancer and the CNS. *Anticancer Agents Med Chem* **10:**625-633.

Robey RW, Pluchino KM, Hall MD, Fojo AT, Bates SE, and Gottesman MM (2018) Revisiting the role of ABC transporters in multidrug-resistant cancer. *Nat Rev Cancer* **18:**452-464.

Robey RW, Shukla S, Finley EM, Oldham RK, Barnett D, Ambudkar SV, Fojo T, and Bates SE (2008) Inhibition of P-glycoprotein (ABCB1)- and multidrug resistance-associated protein 1 (ABCC1)-mediated transport by the orally administered inhibitor, CBT-1((R)). *Biochem Pharmacol* **75:**1302-1312.

Robey RW, Steadman K, Polgar O, Morisaki K, Blayney M, Mistry P, and Bates SE (2004) Pheophorbide a is a specific probe for ABCG2 function and inhibition. *Cancer Res* **64:**1242-1246.

Sparreboom A, van Asperen J, Mayer U, Schinkel AH, Smit JW, Meijer DK, Borst P, Nooijen WJ, Beijnen JH, and van Tellingen O (1997) Limited oral bioavailability and active epithelial excretion of paclitaxel (Taxol) caused by P-glycoprotein in the intestine. *Proc Natl Acad Sci U S A* **94:**2031-2035.

Sugano T, Seike M, Noro R, Soeno C, Chiba M, Zou F, Nakamichi S, Nishijima N, Matsumoto M, Miyanaga A, Kubota K, and Gemma A (2015) Inhibition of ABCB1 Overcomes Cancer Stem Cell-like Properties and Acquired Resistance to MET Inhibitors in Non-Small Cell Lung Cancer. *Mol Cancer Ther* **14:**2433-2440.

Tang SC, Lagas JS, Lankheet N, Rosing H, Beijnen JH, and Schinkel AH (2010) P-glycoprotein (ABCB1) and breast cancer resistance protein (ABCG2) limit sunitinib brain accumulation which can be enhanced by oral elacridar treatment. *Proc Amer Assoc Can Res* **51**.

Thiebaut F, Tsuruo T, Hamada H, Gottesman MM, Pastan I, and Willingham MC (1987) Cellular localization of the multidrug resistance gene product P-glycoprotein in normal human tissues. *Proc Natl Acad Sci U S A* **84:**7735-7738.

van Hoppe S, Sparidans RW, Wagenaar E, Beijnen JH, and Schinkel AH (2017) Breast cancer resistance protein (BCRP/ABCG2) and P-glycoprotein (P-gp/ABCB1) transport afatinib and restrict its oral availability and brain accumulation. *Pharmacol Res* **120:**43-50.

Wall VE, Garvey LA, Mehalko JL, Procter LV, and Esposito D (2014) Combinatorial assembly of clone libraries using site-specific recombination. *Methods Mol Biol* **1116:**193-208.

Wilson CS, Davidson GS, Martin SB, Andries E, Potter J, Harvey R, Ar K, Xu Y, Kopecky KJ, Ankerst DP, Gundacker H, Slovak ML, Mosquera-Caro M, Chen IM, Stirewalt DL, Murphy M, Schultz FA, Kang H, Wang X, Radich JP, Appelbaum FR, Atlas SR, Godwin J, and Willman CL (2006) Gene expression profiling of adult acute myeloid leukemia identifies novel biologic clusters for risk classification and outcome prediction. *Blood* **108:**685-696.

Yang JJ, Milton MN, Yu S, Liao M, Liu N, Wu JT, Gan L, Balani SK, Lee FW, Prakash S, and Xia CQ (2010) P-glycoprotein and breast cancer resistance protein affect disposition of tandutinib, a tyrosine kinase inhibitor. *Drug Metab Lett* **4:**201-212.

Zaher H, Khan AA, Palandra J, Brayman TG, Yu L, and Ware JA (2006) Breast cancer resistance protein (Bcrp/abcg2) is a major determinant of sulfasalazine absorption and elimination in the mouse. *Mol Pharm* **3:**55-61.

Footnote

This research was supported in part by the Intramural Research Program of the National

Institutes of Health, the National Cancer Institute.

FIGURE LEGENDS

Fig. 1. Characterization of ABCB1 and ABCG2 expression in transfected HEK-293 cells. (A)

Trypsinized cells were incubated with phycoerythrin-labeled UIC2 antibody (to detect ABCB1),

5D3 antibody (to detect ABCG2) or the appropriate isotype control for 20 min in 2% BSA after

which cells were washed in PBS and read on a flow cytometer. Untreated cells (cell

autofluorescence, Control) are denoted by the red curve, cells incubated with the isotype

control are denoted by the blue curve, and cells incubated with the specific transporter

antibodies are denoted by the orange curve. (B) Whole cell lysates were subjected to PAGE and

transferred to a nitrocellulose membrane which was subsequently probed with antibodies to

ABCB1 (UIC2), ABCG2 (BXP-21) and GAPDH which served as a loading control. MDR-19 cells

served as a positive control for ABCB1, while R-5 cells were a positive control for ABCG2. Near

infrared-tagged secondary antibodies allowed for protein detection and band intensity was

measured on a Li-COR Odyssey scanner.

Fig. 2. Characterization of ABCB1 and ABCG2 function in transfected HEK-293 cells. (A)

Trypsinized cells were incubated with rhodamine 123 (0.5 µg/ml) or pheophorbide A (2 µm) in

the absence or in the presence of a protein-specific inhibitor (3 µM valspodar for ABCB1; 10 µM

FTC for ABCG2) for 30 min after which media was removed and replaced with substrate free

medium continuing with or without the inhibitor for an additional 1 h. Intracellular substrate

fluorescence was measured with a FACSCanto II flow cytometer. Control cells (cell

autofluorescence) are denoted by the red curve, cells incubated with the substrate alone are

25

denoted by the blue curve and cells incubated with the substrate and inhibitor are denoted by the orange curve.

Fig. 3. ABCB1- and ABCG2-expressing cells are resistant to both ABCB1 and ABCG2 substrates. Three day cytotoxicity assays were performed on empty-vector transfected cells (PEL), *ABCB1*-transfected cells (B1), *ABCG2*-transfected cells (G2), or vector containing both genes (B1/G2) with mitoxantrone, doxorubicin, topotecan, and prexasertib. IC$_{50}$ values were obtained and are summarized in Table 1.

Fig. 4. ABCB1 and ABCG2 can independently transport specific fluorescent substrates. Trypsinized cells were incubated with 0.5 μg/ml rhodamine alone or in combination with 2 μm pheophorbide a in the absence or presence of 3 μg/ml of the ABCB1 inhibitor valspodar, 10 μM of the ABCG2 inhibitor FTC, or both for 30 min. Subsequently, cells were incubated with substrate-free medium continuing without or with inhibitiors for an additional 1 h. Intracellular fluorescence in the presence of the substrates only is denoted by the orange histogram, while fluorescence in the presence of the inhibitors is denoted by the blue histogram. Cell autofluoresence (untreated cells) is denoted by the red histogram. Results from one of three experiments are shown. (A) Top row, cells incubated with rhodamine alone using valspodar as the inhibitor; bottom row, cells incubated with rhodamine and PHA simultaneously using both valspodar and FTC as the inhibitors. Rhodamine fluorescence was examined using a 488 nm laser. (B) Top row, cells incubated with PHA alone; bottom row, cells incubated with rhodamine

and PHA simultaneously using both valspodar and FTC as the inhibitors. PHA fluorescence was

examined using a 650 nm laser.

Fig. 5. ABCB1 and ABCG2 additively transport common substates. Trypsinized cells were

incubated with 250 nM BODIPY-prazosin or 10 μm mitoxantrone in the absence (blue line) or

presence of 3 μg/ml of the ABCB1 inhibitor valspodar (orange line), 10 μM of the ABCG2

inhibitor FTC (green line), or both inhibitors (purple line). Rhodamine fluorescence was

measured using the 488 nm laser and mitoxantrone fluorescence was measured using the 650

nm laser. Results from one of three experiments are shown.

Fig. 6. ABCB1 and ABCG2 confer additive resistance to common substrates. Four day

cytotoxicity assays were performed on PEL or B1/G2 cells with (A) mitoxatrone or (B)

prexasertib in the absence or presence of 3 μg/ml valspodar, 10 μM FTC or both. Results from

one of 3 experiments are shown and results are summarized in Table 2.

Fig. 7. ABCG2 expression diminishes the ability of tariquidar to inhibit ABCB1. (A) B1 or (B)

B1/G2 cells were incubated with 0.5 μg/ml rhodamine 123 in the absence or presence of

increasing concentrations of tariquidar (10 nM, 25 nM, 100 nM, 250 nM) for 30 min after which

the medium was remove and replaced with substate-free medium continuing without or with

the inhibitor. Results from one of three experiments are shown. (C) Results from the three

experiments are summarized and presented as % of total inhibition (afforded by 3 μM

valspodar).

TABLE 1

Summary of cytotoxicity data with PEL, B1, G2 and B1/G2 cells

Drug (µM)	PEL	B1	RR	G2	RR	B1/G2	RR
Mitoxantrone	0.011±0.0036	0.17±0.030	15	0.66±0.35	60	0.27±0.13	24
Doxorubicin	0.022±0.011	1.6±0.50	73	0.086±0.053	4	1.2±0.54	55
Topotecan	0.0034±0.0019	0.011±0.0077	3	0.18±0.078	23	0.065±0.031	19
Prexasertib	3.7±0.58	78±19	21	85±19	23	43±4.6	12

Results presented are IC_{50} +/- standard deviation of at least 3 independent experiments.

Relative resistance (RR) values were determined by dividing the IC_{50} of the transporter-

expressing cells by the IC_{50} for the PEL cells.

TABLE 2

Summary of cytotoxicity data examining the contribution of ABCB1 and ABCG2 to resistance to mitoxantrone and prexasertib

Drug (µM)	PEL	PEL + Val	PEL + FTC	PEL + Val + FTC	B1/G2	B1/G2 + Val	B1/G2 + FTC	B1/G2 + Val + FTC
Mitoxantrone	0.006±0.002	0.004±0.0005	0.008±0.001	0.004±0.0005	0.3±0.06	0.1±0.08	0.2±0.1	0.01±0.0005
Prexasertib	2.2±0.043	1.8±0.16	1.9±0.094	1.8±0.12	13±8.6	12±2.1	16±3.5	5.5±3.9

Results presented are IC$_{50}$ +/- standard deviation of at least 3 independent experiments.
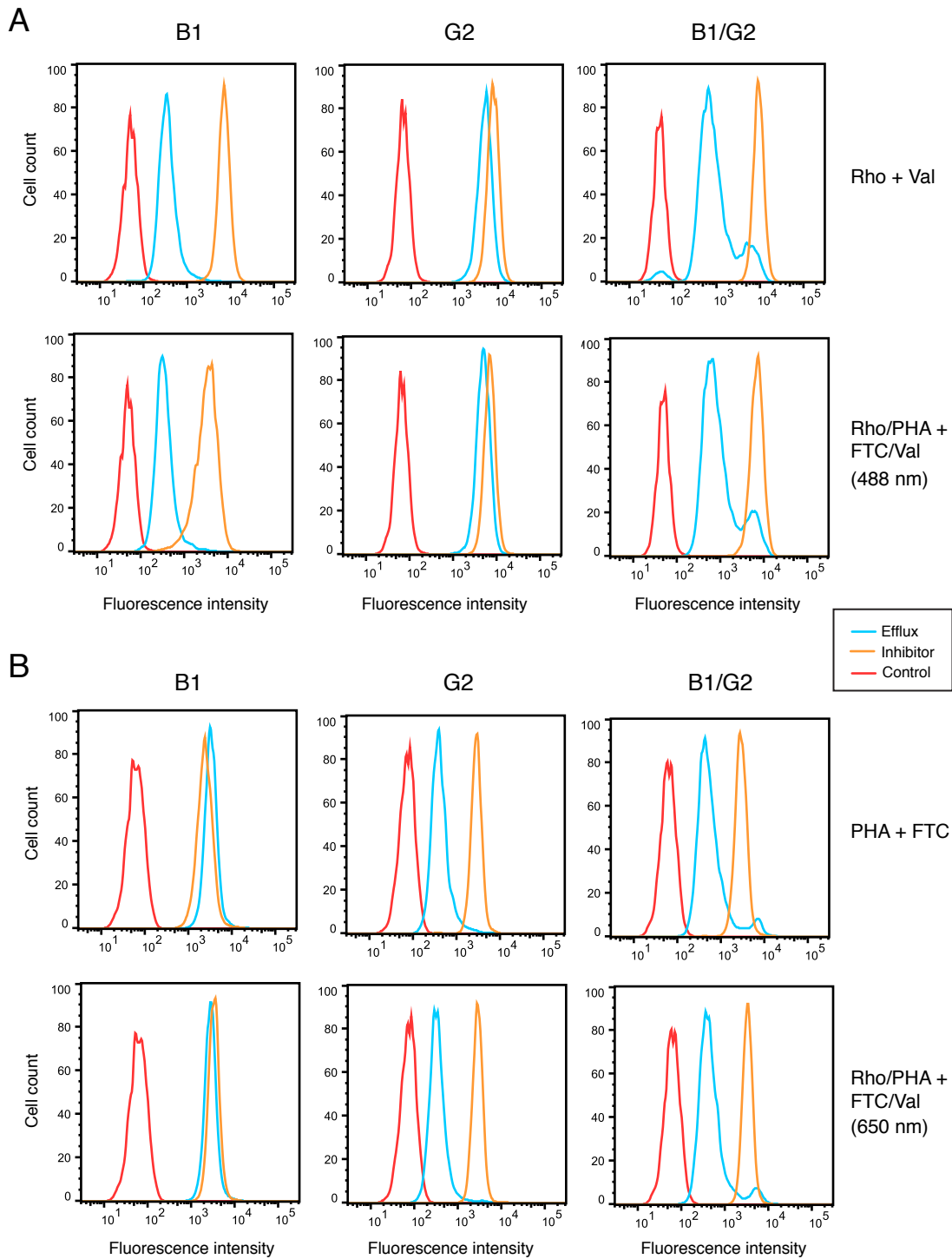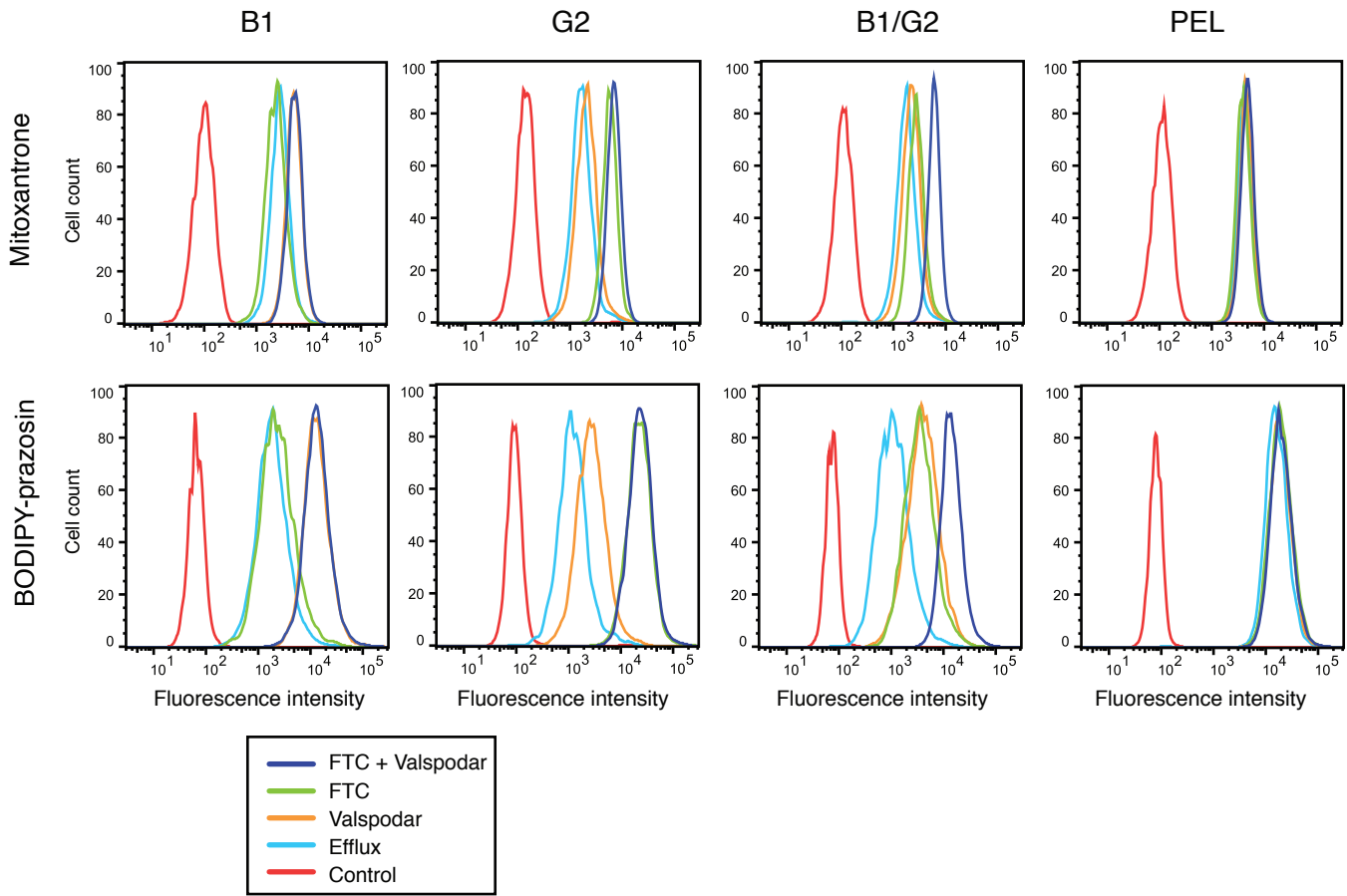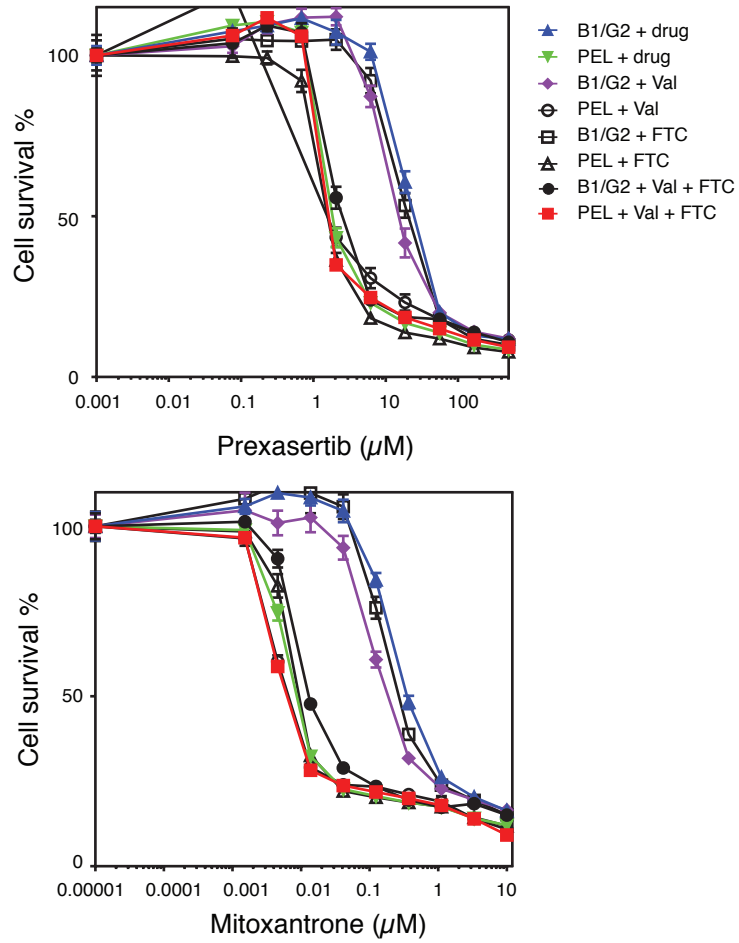
Figure 1
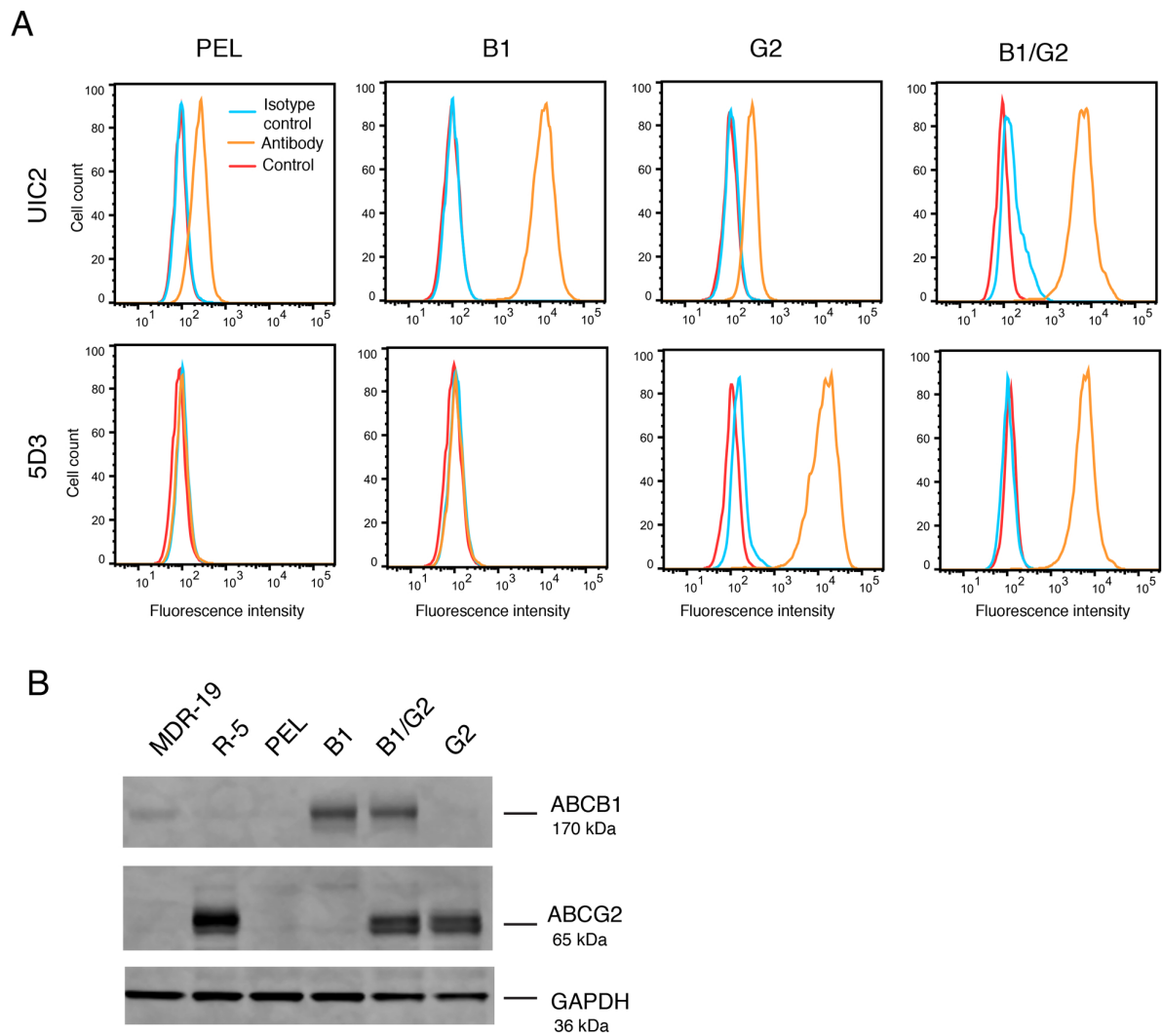
Figure 2
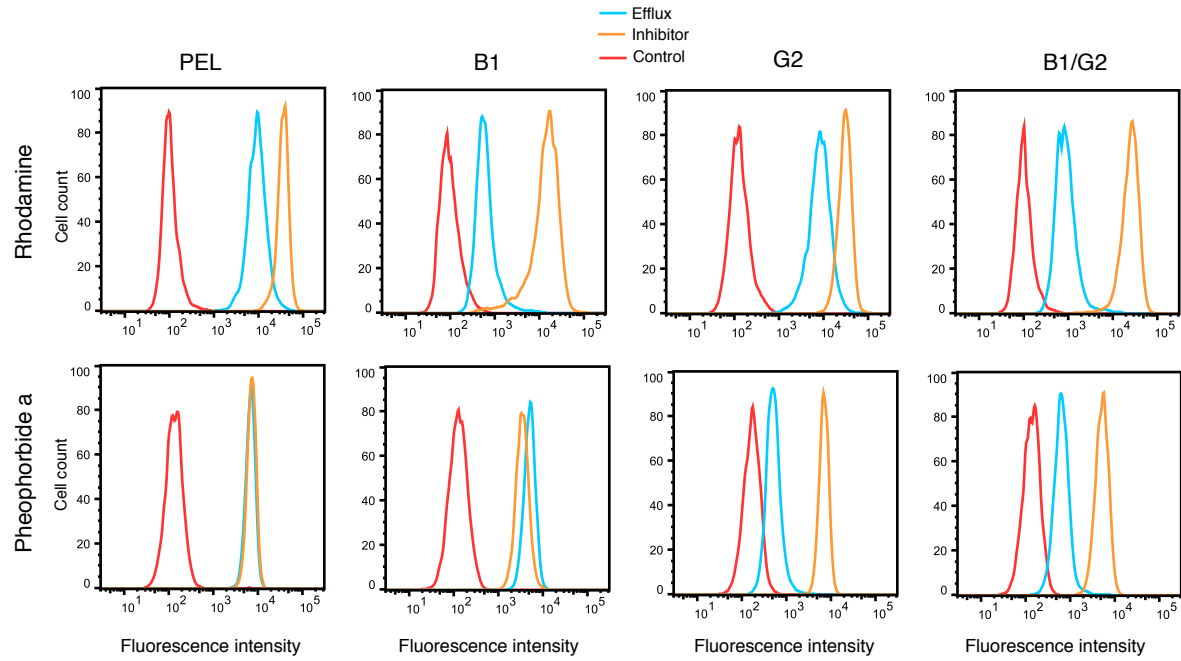
Figure 3
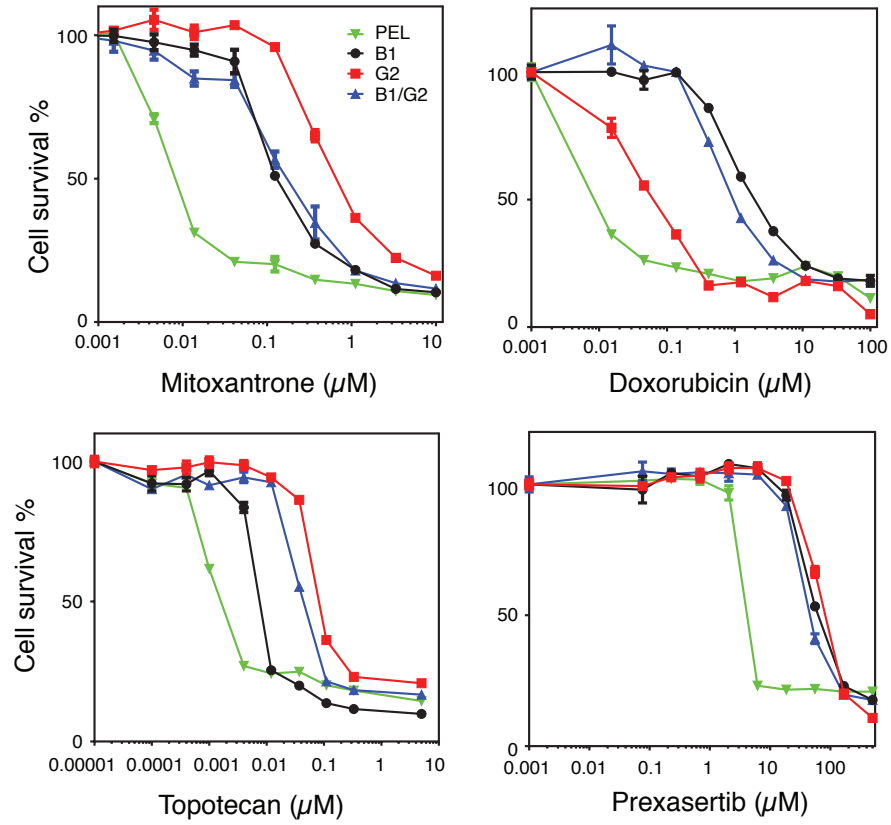
Figure 4

Figure 5

Figure 6

Figure 7